

# Compressing KV Cache for Long-Context LLM Inference with Inter-Layer Attention Similarity

Da Ma<sup>1</sup>, Lu Chen<sup>1\*</sup>, Situo Zhang<sup>1</sup>, Yuxun Miao<sup>1</sup>, Su Zhu<sup>2</sup> Zhi Chen<sup>2</sup> Hongshen Xu<sup>1</sup>  
Hanqi Li<sup>1</sup>, Shuai Fan<sup>3</sup>, Lei Pan<sup>3</sup>, Kai Yu<sup>1\*</sup>

<sup>1</sup>X-LANCE Lab, Department of Computer Science and Engineering  
MoE Key Lab of Artificial Intelligence, SJTU AI Institute  
Shanghai Jiao Tong University, Shanghai, China  
<sup>2</sup>ByteDance <sup>3</sup>AISpeech Co., Ltd., Suzhou, China  
mada123@sjtu.edu.cn

## Abstract

The rapid expansion of context window sizes in Large Language Models (LLMs) has enabled them to tackle increasingly complex tasks involving lengthy documents. However, this progress comes at the cost of a substantial increase in memory usage during inference, primarily due to the linear growth of the key-value (KV) cache. Existing KV cache compression methods often discard less relevant tokens, which can lead to significant performance degradation when critical information is lost. In this paper, we propose POD (Proximal tokens over Distant tokens), a novel KV cache compression framework that allocates memory according to token importance, retaining less important tokens in a more compact, shared form rather than discarding them entirely. Our approach is motivated by two key observations: (1) proximal tokens—those at the beginning and end of the context—are significantly more important for next-token prediction, and (2) attention scores for distant tokens are highly redundant across consecutive layers. Leveraging these insights, POD preserves the full KV cache for proximal tokens, while for distant tokens, it shares key states across layers. Since attention scores are determined by both queries and keys, sharing key states enables multiple layers to reuse a single set of keys for distant tokens, substantially reducing KV cache memory without discarding essential context. We further introduce a lightweight post-training adaptation to enable the model to adjust to this new attention-sharing structure. Extensive experiments on both synthetic (Needle in a Haystack) and real-world long-context benchmarks demonstrate that POD reduces KV cache memory usage by up to 35% without compromising performance. Our method is orthogonal to existing token-selection-based techniques and can be combined with them for further KV cache compression.

## 1 Introduction

Recently, the increasing context window size in Large Language Models (LLMs) (Brown et al. 2020; Achiam et al. 2023; Team et al. 2023; Reid et al. 2024; Touvron et al. 2023a,b; Dubey et al. 2024) has allowed them to handle complex tasks requiring in-depth exploration of lengthy texts (Bairi et al. 2024; Mazumder and Liu 2024). However, it poses challenges to the memory footprint during inference. Specifically, since most LLMs are based on the Trans-

former (Vaswani et al. 2017) architecture, the size of key-value (KV) cache (Pope et al. 2023), a widely used technique designed to prevent redundant computations, grows linearly with the context window size. Hence, compressing the KV cache during inference has become a critical problem for deploying LLMs with long context windows.

Against this backdrop, recent studies have explored compressing the KV cache during inference by discarding less relevant tokens from the context. For example, window attention (Beltagy, Peters, and Cohan 2020) keeps only the most recent tokens, while methods such as LM-Infinite (Han et al. 2024), StreamingLLM (Xiao et al. 2024) and H<sub>2</sub>O (Zhang et al. 2023) further refine which tokens to retain based on their positional or contextual importance. Although these approaches effectively reduce memory usage, they share a common drawback (Tang et al. 2024): *critical tokens needed for subsequent text generation may be prematurely discarded*, leading to significant performance degradation when important information falls outside the cache. As shown in Figure 1-(a), when the important tokens (evidence in the example) fall outside the cache (the blue segment), the prediction fails. This limitation is further evidenced by the performance degradation of StreamingLLM and H<sub>2</sub>O on two real-world benchmarks (see Figure 1-(b)).

In this paper, rather than simply discarding tokens to compress the KV cache, we propose a more nuanced approach that aims to minimize performance degradation while reducing memory usage. Our core motivation is that *less important tokens should occupy less space in the KV cache, rather than being discarded entirely*. This perspective moves beyond hard pruning to retaining less important tokens in a more compact form, which raises two key questions: 1) how to identify, in a probabilistic sense, which tokens are more important for future generation, and 2) how to store less important tokens in a more compact form within the KV cache.

To address these questions, we examine two key properties of LLMs in long-context scenarios:

- **Observation 1:** *Proximal tokens (i.e., initial and recent tokens) are, in a probabilistic sense, substantially more important for next-token prediction than distant tokens.* Our empirical analysis on modern LLMs quantifies this: for 80% of input positions, attending only to the 256 nearest tokens leads to the same prediction as attending

\*Corresponding authors.

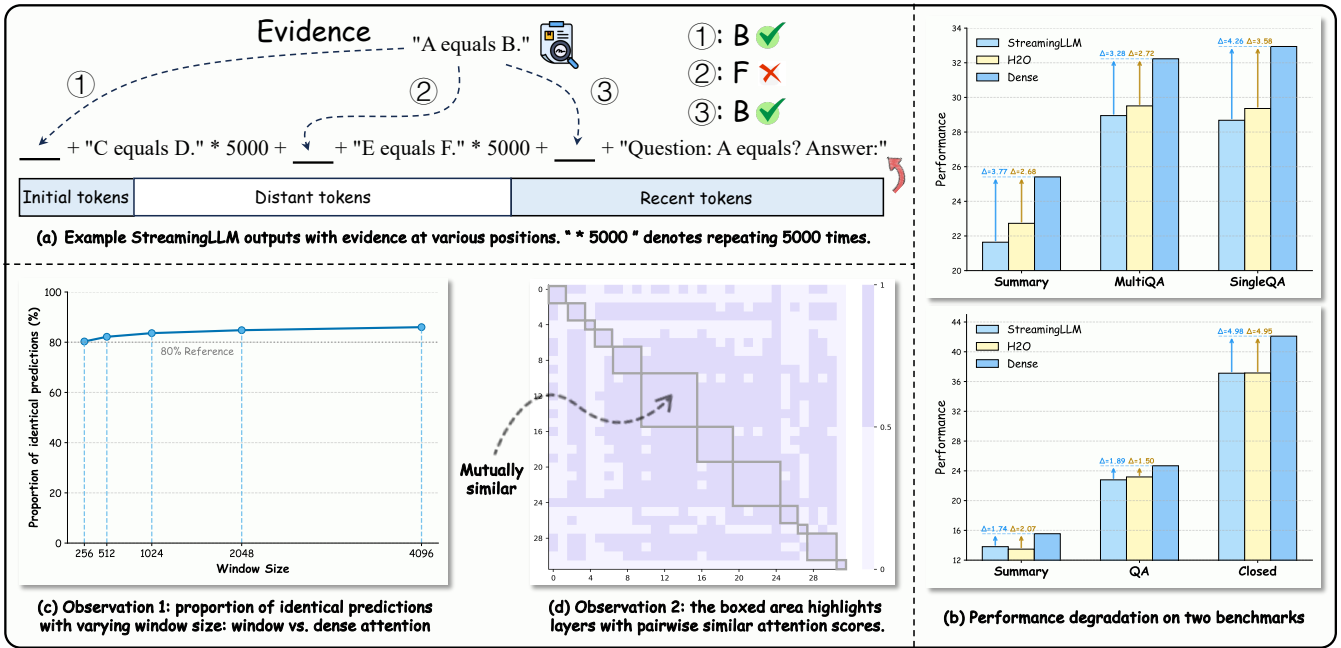


Figure 1: Experimental results from the LLaMA3-8B-32K model, including: (a) prediction failure example, (b) benchmark performance (Details are in § 3.1.), (c) window size impact on prediction consistency (Details are in Appendix B.1.), and (d) attention similarity between layers (Details are in Appendix B.2.).

to the full context (see Figure 1-(c)).

- **Observation 2:** *Attention scores between consecutive layers are highly similar.* While this phenomenon has been reported in smaller models (Xiao et al. 2019; Bhojanapalli et al. 2021), we show that it also holds for modern LLMs. As illustrated in Figure 1-(d), attention scores for distant tokens remain strongly correlated between adjacent layers (see the gray box), indicating substantial inter-layer redundancy.

Building on these two observations, we propose POD (Proximal tokens over Distant tokens) for substantial KV cache compression in long-context LLMs. Motivated by the greater importance of proximal tokens (Observation 1) and the inter-layer redundancy of attention scores for distant tokens (Observation 2), POD preserves the full KV cache for proximal tokens, while sharing attention scores across layers for distant tokens. As attention scores are determined by query and key states, this sharing enables multiple layers to reuse a single set of key states for distant tokens, substantially reducing KV cache memory without discarding essential context. Based on these principles, POD operates in two main stages: 1) *Exploration of Offline Inter-Layer Attention Sharing* (§ 2.1): determining which layers are suitable for sharing attention scores; 2) *Lightweight Training Adaptation* (§ 2.2): post-training the model on a limited dataset to adapt to the identified attention sharing patterns.

In addition, we conducted extensive experiments on Needle in a Haystack and three real-world long-context benchmarks. Results show that POD reduces KV cache memory usage by up to 35% without compromising model perfor-

mance (§ 3). In summary, our main contributions are: 1) proposing a new KV cache compression paradigm that allocates memory based on token importance instead of discarding less important tokens; 2) developing POD, which compresses the KV cache by sharing key states for distant tokens across layers, leveraging inter-layer attention redundancy; and 3) demonstrating that POD achieves up to 35% KV cache memory reduction with no performance loss. We will open-source our code and models.

## 2 Methodology

Our approach (PoD) consists of two main steps: (1) grouping consecutive layers into blocks based on attention similarity analysis, and (2) sharing key states for distant tokens within each block, followed by lightweight post-training adaptation. We describe each step in detail below.

### 2.1 Offline Inter-Layer Attention Sharing Exploration

To guide the application of attention sharing, we first analyze the similarity of attention scores between layers in the LLM. This analysis enables us to group consecutive layers with similar attention patterns into blocks, which serve as the foundation for our sharing strategy.

**Attention Score Calculation** Given  $N$  input sequences  $\{\mathbf{s}_i = (x_1, x_2, \dots, x_n)\}_{i=1}^N$ , we feed each sequence into the model  $\mathcal{M}$  and extract the attention scores for the last  $q$  tokens ( $1 \leq q \leq n$ ) at every layer and attention head. For-

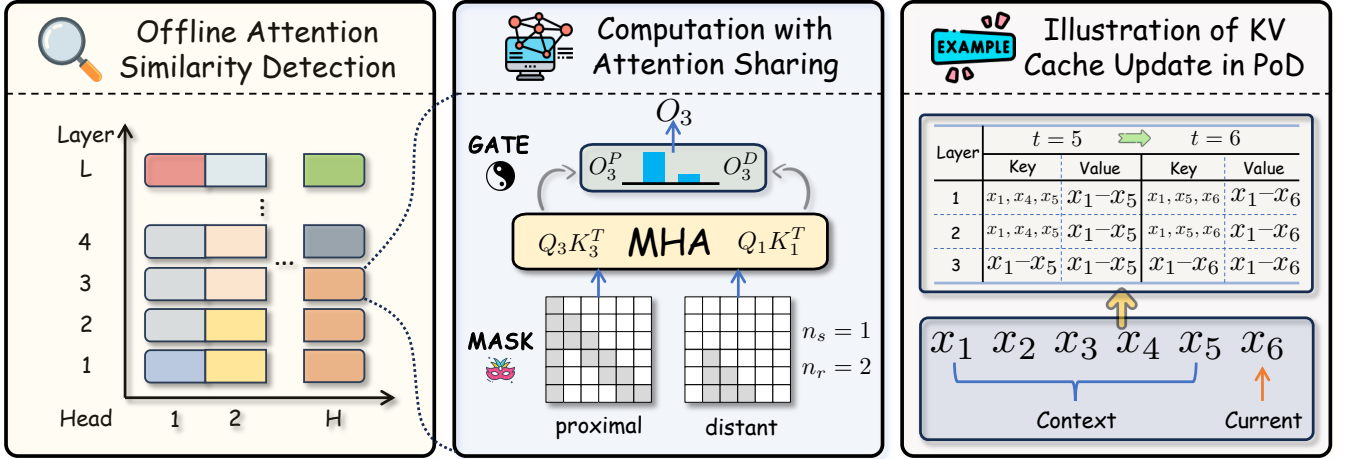


Figure 2: Overview of the POD framework. **Left:** Example of head-wise layer partitioning based on inter-layer attention similarity; **Middle:** Key states for distant tokens are shared across layers within each block to reduce KV cache memory; **Right:** Example of KV cache update in POD.

mally, for each sample, we obtain

$$\left\{ \mathbf{S}_i^{\ell,h} \right\}_{1 \leq \ell \leq L, 1 \leq h \leq H} = \mathcal{M}(\mathbf{s}_i), \quad (1)$$

where  $L$  and  $H$  denote the number of layers and attention heads, respectively, and  $\mathbf{S}_i^{\ell,h} \in \mathbb{R}^{q \times n}$  represents the attention scores at layer  $\ell$  and head  $h$  for the  $i$ -th input.

**Attention Similarity Measurement** To quantify the similarity between any two layers  $\ell_a$  and  $\ell_b$  ( $1 \leq \ell_a, \ell_b \leq L$ ,  $\ell_a \neq \ell_b$ ) for a given head  $h$ , we compute the average Jensen-Shannon (JS) divergence (Menéndez et al. 1997) between their attention score distributions over the last  $q$  tokens, aggregated across all  $N$  samples:

$$\text{sim}_h(\ell_a, \ell_b) = \frac{1}{Nq} \sum_{i=1}^N \sum_{j=1}^q \text{JS} \left( \mathbf{S}_{i,j}^{\ell_a,h}, \mathbf{S}_{i,j}^{\ell_b,h} \right), \quad (2)$$

where  $\mathbf{S}_{i,j}^{\ell,h}$  denotes the  $j$ -th row of  $\mathbf{S}_i^{\ell,h}$ , corresponding to the attention distribution of the  $j$ -th token in the  $i$ -th input. The similarity score  $\text{sim}_h(\ell_a, \ell_b)$  ranges from 0 (completely dissimilar) to 1 (identical).

**Layer Grouping Strategy** Based on the computed head-wise attention similarities, we group consecutive layers into blocks such that all layers within a block are sufficiently similar. Specifically, we consider two layers to be similar if  $\text{sim}_h(\ell_a, \ell_b) \geq 0.5$ . For each head, we employ a bottom-up greedy algorithm to iteratively merge consecutive similar layers into blocks, as detailed in Algorithm 1. The resulting head-wise layer partitioning is exemplified in Figure 2 (left).

## 2.2 Lightweight Training Adaptation

To ensure the model can adapt to the new attention sharing mechanism within each block, we perform a lightweight post-training adaptation.

**Attention Sharing within Each Block** Let  $\mathbf{s} = (x_1, x_2, \dots, x_n)$  denote a long input sequence. In standard autoregressive Transformer-based LLMs, each token  $x_i$  ( $1 \leq i \leq n$ ) at layer  $\ell$  attends to all previous tokens  $\{x_j\}_{j \leq i}$ . To reduce the memory and computation costs associated with distant tokens, we divide the preceding tokens into two groups: proximal tokens and distant tokens. Following prior works (Han et al. 2024; Xiao et al. 2024), we treat both the most recent tokens and several initial tokens as proximal tokens, accounting for the ‘‘attention sink’’ phenomenon. Each token  $x_i$  attends to both groups; however, for distant tokens, all layers within a block share the attention scores computed at the lowest layer of the block identified in Section 2.1.

Mathematically, for any attention head, let  $\mathbf{Q}_\ell, \mathbf{K}_\ell, \mathbf{V}_\ell \in \mathbb{R}^{n \times d}$  denote the query, key, and value matrices at the  $\ell$ -th layer, respectively\*. Suppose layer  $\ell$  belongs to block  $B_\ell = \{\bar{\ell} \mid \ell_a \leq \bar{\ell} \leq \ell_b\}$ , which consists of consecutive layers. For a given token  $x_i$ , we partition the preceding tokens into proximal and distant groups as described above. The attention outputs for  $x_i$  with respect to proximal and distant tokens are computed as follows<sup>†</sup>:

$$\begin{aligned} \mathbf{a}_{\ell,i}^P &= \frac{\mathbf{Q}_{\ell,i} [\mathbf{K}_{\ell,[1,n_s]}; \mathbf{K}_{\ell,[n-n_r+1,n]}]^T}{\sqrt{d}}, \\ \mathbf{o}_{\ell,i}^P &= \text{Softmax}(\mathbf{a}_{\ell,i}^P) [\mathbf{V}_{\ell,[1,n_s]}; \mathbf{V}_{\ell,[n-n_r+1,n]}], \\ \mathbf{a}_{\ell,i}^D &= \frac{\mathbf{Q}_{\ell_a,i} \mathbf{K}_{\ell_a,[n_s+1,n-n_r]}^T}{\sqrt{d}}, \\ \mathbf{o}_{\ell,i}^D &= \text{Softmax}(\mathbf{a}_{\ell,i}^D) \mathbf{V}_{\ell,[n_s+1,n-n_r]}, \end{aligned} \quad (3)$$

where  $\mathbf{Q}_{\ell,i}$  denotes the  $i$ -th row of  $\mathbf{Q}_\ell$ , and  $\mathbf{K}_{\ell,[a,b]}$  denotes the rows from  $a$  to  $b$  (inclusive) of  $\mathbf{K}_\ell$ . Here,  $n_s$  (start

\*For simplicity, we omit the attention head subscripts.

<sup>†</sup>If there are no distant tokens for  $x_i$ , the corresponding attention term is omitted.

---

**Algorithm 1: Greedy Layer Grouping Algorithm**

---

**Input:** Head-wise attention similarities between layers:  $\{sim_h(\ell_a, \ell_b)\}_{1 \leq h \leq H, 1 \leq \ell_a, \ell_b \leq L}$   
**Output:** Head-wise layer blocks  
head\_wise\_layer\_blocks  $\leftarrow []$ ;  
**for** head  $h \leftarrow 1$  **to**  $H$  **do**  
  current\_head\_layer\_blocks  $\leftarrow [\{1\}]$ ;   // Each block is a set.  
  **for** layer  $\ell \leftarrow 2$  **to**  $L$  **do**  
    current\_block  $\leftarrow$  the last element of current\_head\_layer\_blocks;  
    // Layer  $\ell$  is similar to all layers in the current block.  
    **if**  $sim_h(\ell, \hat{\ell}) \geq 0.5, \forall \hat{\ell} \in$  current\_block **then**  
      Add  $\ell$  to current\_block;  
    **else**  
      Append  $\{\ell\}$  to current\_head\_layer\_blocks;  
  Append current\_head\_layer\_blocks to head\_wise\_layer\_blocks;  
**Return** head\_wise\_layer\_blocks;

---

size) and  $n_r$  (recent size) represent the number of initial and most recent tokens classified as proximal tokens, respectively, and  $[\cdot; \cdot]$  denotes concatenation.  $\mathbf{a}_{\ell,i}^P \in \mathbb{R}^{1 \times (n_s + n_r)}$  and  $\mathbf{o}_{\ell,i}^P \in \mathbb{R}^{1 \times d}$  are the attention logits and outputs for proximal tokens, respectively; analogous notations apply to distant tokens.

**Aggregation of Attention Outputs to Proximal and Distant Tokens** To combine the attention outputs from proximal and distant tokens, we employ a parameter-free gating mechanism<sup>‡</sup>:

$$g_{\ell,i} = \frac{\sum \exp \mathbf{a}_{\ell,i}^P}{\sum \exp \mathbf{a}_{\ell,i}^P + \sum \exp \mathbf{a}_{\ell,i}^D}, \quad (4)$$
$$\mathbf{o}_{\ell,i} = g_{\ell,i} \cdot \mathbf{o}_{\ell,i}^P + (1 - g_{\ell,i}) \cdot \mathbf{o}_{\ell,i}^D,$$

where  $g_{\ell,i}$  adaptively balances the contributions from proximal and distant tokens for each token  $x_i$  at layer  $\ell$ . Figure 2 (middle) provides a detailed example of the computation under the attention sharing scheme, highlighting the attention masks applied to proximal and distant tokens.

### 3 Experiments

In this section, we mainly address two key questions:

- Does POD maintain model performance in long-context scenarios?
- Can POD effectively reduce KV cache memory usage during long-context inference?

---

<sup>‡</sup>The derivation of the gating formula is provided in Appendix C.1.

**Implementation Details** For data preparation, we sampled 5B tokens from Dolma (Soldaini et al. 2024) for post-training, ensuring that the number of tokens in each sequence length interval remains consistent (GLM et al. 2024).

The baseline model, LLaMA3-8B-32K, was obtained by post-training LLaMA3-8B on 5B tokens with a maximum sequence length of 32K. To construct the POD model, we first performed offline attention similarity detection on LLaMA3-8B-32K (see Appendix B.2 for details) to determine the optimal layer grouping for attention sharing, which resulted in approximately 35% KV cache memory savings. Subsequently, we continued post-training from LLaMA3-8B-32K on the same 5B tokens (with a maximum sequence length of 32K), applying the new attention sharing structure with  $n_s = 16$  and  $n_r = 4080$ , to adapt the model to these architectural changes.

During training, we used a batch size of 4M tokens and set the learning rate to  $1e-5$  with a cosine annealing scheduler. The RoPE (Rotary Positional Embedding) (Su et al. 2023) base was set to 16M+, following the approach of (Xiong et al. 2024). For implementation, we adopted the HuggingFace (Wolf et al. 2020) and DeepSpeed (Rasley et al. 2020) frameworks, incorporating ZeRO-3 (Rajbhandari et al. 2020) and Ulysses (Jacobs et al. 2023) sequence parallelism. Additionally, we employed the efficient FlexAttention module from PyTorch (Paszke et al. 2019).

**Baselines** We consider three types of baselines:

- *Token-selection-based methods:* SnapKV (Li et al. 2024) selects and caches important tokens based on attention scores during prefilling. PyramidKV (Zhang et al. 2024b) extends SnapKV by varying the number of cached tokens across layers. Quest (Tang et al. 2024) does not reduce KV cache size, but decreases the number of tokens involved in attention computation via efficient token selection.
- *Token-eviction-based methods:* Window Attention (WA) (Beltagy, Peters, and Cohan 2020) restricts each token to attend only to a local window. WA+CPT further post-trains the model with window attention. StreamingLLM (Xiao et al. 2024) and LM-Infinite (Han et al. 2024) allow tokens to attend to both neighboring and initial tokens, with LM-Infinite using different position embeddings. H<sub>2</sub>O dynamically adds or removes tokens based on attention scores during decoding.
- *Layer-sharing-based methods:* CLA (Brandon et al. 2024) reduces KV cache by sharing key and value states across adjacent layers.

More details are in Appendix A.

#### 3.1 Performance Evaluation

To evaluate the performance of POD, we conducted experiments in two fields: 1) Needle in a Haystack and 2) Practical Long Context Benchmarks.

**Needle in a Haystack** Table 2 presents a quantitative comparison of different methods on the needle-in-a-haystack task, where a random statement (the “needle”) is placed

Model	Window	LongBench						LEval			
		SQA	MQA	Summ	Few-Shot	Code	Avg.	Closed	QA	Summ	Avg.
LLaMA3-8B-32K	32K	32.9	32.2	25.4	69.3	66.5	45.3	42.1	24.7	15.6	27.5
<b>Token-selection-based methods</b>											
SnapKV	4K	31.8	31.9	21.9	68.6	66.7	44.2	39.9	23.9	13.5	25.8
PyramidKV	4K	33.3	31.5	23.8	68.9	66.4	44.8	42.1	22.6	13.0	25.9
Quest	4K	32.1	32.2	24.3	69.1	66.4	44.8	40.6	25.6	14.7	26.9
<b>Token-eviction-based methods</b>											
LM-Infinite	16+4080	28.8	29.0	21.7	68.1	66.5	42.8	37.3	22.8	13.9	24.7
StreamingLLM	16+4080	28.7	29.0	21.6	68.1	66.6	42.8	37.1	22.8	13.8	24.6
H <sub>2</sub> O	96+4000	29.4	29.5	22.7	68.5	66.2	43.2	37.2	23.2	13.5	24.6
WA	4K	8.9	3.6	9.1	11.1	41.1	14.8	21.0	5.6	2.8	9.8
WA+CPT	4K	26.9	28.0	22.3	66.6	66.1	42.0	32.9	22.1	12.6	22.5
<b>Layer-sharing-based methods</b>											
CLA	32K	24.0	22.6	22.5	60.9	59.4	37.9	19.1	13.5	11.5	14.7
PoD (ours)	16+4080+28K	31.0	32.4	24.8	67.3	68.3	44.8	43.6	23.0	15.0	27.2
PoD+SnapKV (ours)	4K	31.0	32.7	22.9	66.9	67.8	44.3	43.1	22.1	14.3	26.5

Table 1: Evaluation results of different methods on two famous long context benchmarks

Method	Score (%)
Dense	97.9
SnapKV	98.3
PyramidKV	97.8
StreamingLLM	56.8
H <sub>2</sub> O	55.6
CLA	64.8
PoD (ours)	98.9
PoD+SnapKV (ours)	94.6

Table 2: Scores for needle in a haystack

in the middle of a long context window and the model is asked to retrieve it. The results show that PoD and other token-selection-based methods (e.g., SnapKV, PyramidKV) achieve near-perfect performance, significantly outperforming token-eviction-based methods (StreamingLLM, H<sub>2</sub>O) and the layer-sharing-based method (CLA). Notably, PoD and token-selection-based approaches are orthogonal and can be combined, as demonstrated by the strong performance of PoD+SnapKV. The visual illustration of the search results is shown in Appendix B.3.

**Long Context Benchmarks** To ensure that PoD can handle real-world tasks, we evaluated it on two well-known long context benchmarks: LongBench (English version) (Bai et al. 2024) and LEval (An et al. 2024). We test on 14 datasets within LongBench involving Single-document QA, Multi-document QA, Summarization, Few-shot learning, and Code completion tasks. LEval consists of 20 sub-tasks, divided into two groups: closed-domain and open-domain. The closed-domain group primarily evaluates reasoning and comprehension over longer contexts, while the open-domain group focuses on tasks such as summarization and question answering, which require aggregating information from long

Theoretical saving	Practical maximum batch size $b$				
	$x$	$y$	Dense	PoD	↑
35%	2048	8192	25	33	32.0%
	4096	8192	13	17	30.8%
	8192	8192	6	8	33.3%
	16384	8192	3	4	33.3%

Table 3: Theoretical and practical memory footprint savings

documents.

Table 1 illustrates all experimental results. To ensure fairness, all baseline attention mechanisms have the same window size. For PoD, we also ensure that the number of proximal tokens each token attends to is consistent with this window size. We can draw the following conclusions: 1) PoD outperforms token-eviction-based methods, demonstrating that our approach of not losing tokens is indeed effective. 2) With a small amount of post-training data, PoD beats the classical layer-sharing-based method CLA, demonstrating that our model has an advantage in adapting existing LLMs. 3) Both PoD and token-selection-based methods can achieve performance comparable to the standard dense model. Furthermore, PoD is *orthogonal* to token-selection-based methods, and combining them can further reduce the size of the KV cache while maintaining model performance.

### 3.2 Efficiency Evaluation

**KV Cache Memory** The savings in memory consumption can be analyzed from both theoretical and empirical perspectives. Theoretically, we can calculate the potential reduction in KV cache size based on the layer-sharing results obtained from offline analysis. Empirically, we can conduct end-to-end evaluations to assess the actual savings. Following FlexGen (Sheng et al. 2023) and LCKV (Wu and Tu

Model	32K					64K					128K					Avg.
	QA	MC	Summ	PK	NS	QA	MC	Summ	PK	NS	QA	MC	Summ	PK	NS	
LLaMA3.1-8B	29.6	25.3	15.5	27.1	27.1	37.3	28.8	15.1	54.2	54.2	31.2	41.8	14.9	100.0	99.5	40.1
<i>Token-selection-based methods</i>																
SnapKV	28.9	26.2	13.3	27.1	26.6	35.1	28.0	11.7	54.2	53.1	29.3	34.5	13.7	100.0	99.0	38.7
PyramidKV	29.9	26.2	15.0	27.1	27.1	36.5	29.3	15.2	54.2	54.2	OOM <sup>§</sup>			OOM		
Quest	28.5	25.8	12.9	27.1	27.1	35.8	27.5	11.2	54.2	54.2	29.0	34.5	9.0	100.0	98.1	38.3
<i>Token-eviction-based methods</i>																
LM-Infinite	25.3	26.6	12.5	3.4	3.4	27.3	28.8	12.6	3.4	3.4	22.2	29.3	13.0	3.4	3.2	14.5
StreamingLLM	25.4	26.2	12.1	3.4	3.4	27.1	28.0	13.3	3.4	3.4	22.7	28.0	12.8	3.4	3.2	14.4
H <sub>2</sub> O	25.4	26.2	13.1	4.9	3.4	27.6	28.0	14.3	7.1	3.6	OOM <sup>§</sup>			OOM		
WA	3.5	3.5	0.5	0.0	1.4	3.4	3.1	0.7	0.0	1.2	3.3	3.5	0.7	0.0	1.2	1.7
WA+CPT	12.6	18.8	11.3	3.4	3.4	13.1	17.9	10.8	3.4	3.4	12.8	21.0	11.3	3.4	3.4	10.0
<i>Layer-sharing-based methods</i>																
CLA	22.1	34.1	13.6	24.1	25.8	22.7	31.9	12.7	50.9	52.5	21.6	34.5	13.0	97.8	96.8	36.9
PoD	27.4	35.4	17.9	26.6	27.1	29.6	36.9	15.5	53.7	54.2	26.6	42.8	15.5	99.8	99.2	40.6
PoD+SnapKV	28.6	35.9	13.9	26.6	23.4	28.5	36.2	14.0	53.7	49.5	24.7	40.6	12.4	99.8	88.0	38.4

Table 4: Evaluation results on InfiniteBench (128K). OOM: out of memory over one A800-80G GPU

2024), for a prompt of length  $x$ , we let the model generate  $y$  tokens. The maximum batch size  $b$  achievable on a given GPU will be used to assess the memory requirements of the model. A larger  $b$  indicates that the model is more memory-efficient. Table 3 presents the memory consumption results. We observe that PoD achieves a more than 30% increase in maximum batch size across varying input text lengths, closely aligning with our theoretical KV cache savings rate of 35%, demonstrating that PoD effectively reduces memory usage.

**Latency and Efficiency** Table 5 compares various methods in terms of latency (throughput), KV cache savings, and performance. Our analysis highlights clear trade-offs:

- Token-eviction-based methods offer fast throughput and high KV cache savings but incur notable performance loss.
- Token-selection-based methods compress the KV cache with minimal performance impact, but the token selection step slows down inference.
- PoD achieves lower latency than SnapKV while still maintaining strong performance and cache savings, and combining PoD with token-selection-based methods brings further gains across all dimensions.

However, all performance-preserving methods—such as SnapKV, PyramidKV, and PoD—still incur some latency overhead. Improving their efficiency is an important direction for future work.

### 3.3 Additional Analysis

**Scaling to longer context and other LLMs** To explore the generality of our method, we conducted experiments on LLaMA3.1-8B (Dubey et al. 2024), which can handle longer (128K) contexts. We sampled 5B tokens from the ProLong-data-512K (Gao et al. 2024) dataset and applied the same hyperparameter configuration used for training

Method	Stage	Tp ↑	KV ↑ (%)	Perf ↓ (%)
Dense	-	40.3	-	-
<i>Token-selection-based methods</i>				
SnapKV	P	24.5	87.5	4.3
PyramidKV		20.6	93.6	3.4
<i>Token-eviction-based methods</i>				
LM-Infinite	P&D	42.8		7.7
StreamingLLM		43.0		8.0
H <sub>2</sub> O		27.7	87.5	7.4
WA		50.1		65.9
WA+CPT		50.1		12.6
<i>Layer-sharing-based methods</i>				
CLA	P&D	41.8	50.0	31.4
PoD (ours)		31.7	35.0	2.8
PoD+SnapKV (ours)		23.4	91.9	3.1

Table 5: Comparison of different methods from multiple perspectives. **Stage**: optimized stage. ‘P’ indicates Prefilling and ‘D’ indicates Decoding; **Tp**: throughput (tokens per second); **KV**: KV cache saving; **Perf**: performance degradation.

LLaMA3-8B-32K to post-train LLaMA3.1-8B with a sequence length of 128K. The evaluation results over 5 sub-tasks in the InfiniteBench (Zhang et al. 2024a) under different context sizes are shown in Table 4.

Consistent with the conclusions found in Table 1, our method causes less performance degradation compared to token-eviction-based methods. However, a notable difference is that token-selection-based methods appear to struggle in maintaining model performance in longer context scenarios. This limitation is also reflected in the combined model (PoD+SnapKV), which integrates our method with token-selection-based methods, showing a decline in performance. This to some extent indicates that our method is

Method	MMLU	HS	Arc-e	Arc-c	HE	Avg.
Dense	61.4	58.0	80.9	70.2	28.0	59.7
CLA	36.1	52.6	23.0	28.4	14.6	30.9
PoD	62.8	59.7	83.5	73.6	29.3	61.8

Table 6: Results on standard benchmarks. HS and HE denote Hellaswag and HumanEval, respectively.

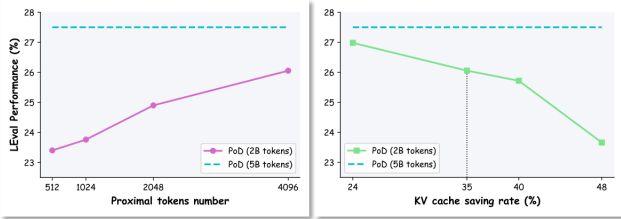


Figure 3: Ablation study on key hyperparameters in POD. **Left:** LEval performance vs. proximal tokens number. **Right:** LEval performance vs. KV cache saving rate. 4K proximal tokens and 35% saving rate provide a good balance of accuracy and KV cache compression rate.

more robust to the context length.

**Ablation Study on Key Hyperparameters in POD** We examine how two key hyperparameters in POD—the number of proximal tokens and the KV cache saving rate—affect model performance. Starting from LLaMA3-8B-32K, we continued training with 2B tokens. As shown in Figure 3 (left), increasing the number of proximal tokens consistently improves performance, with 4K proximal tokens enabling the model to match the performance of LLaMA3-8B-32K trained on 5B tokens. Figure 3 (right) shows that higher KV cache saving rates lead to decreased performance. To strike a balance between KV cache compression and accuracy, we set the number of proximal tokens to 4K and compressed the KV cache to 35%, maintaining competitive performance with reduced resource usage.

**Evaluation on Standard Benchmarks** Table 6 shows model performance on standard benchmarks. POD matches the dense baseline with no accuracy loss, while CLA suffers significant degradation, likely due to indiscriminate information sharing across layers.

**Case Study** Figure 4 compares StreamingLLM, H<sub>2</sub>O, and POD on four representative cases. In case (a), the answer is within the window of recent tokens, so all methods make correct predictions. In case (b), the answer is at the beginning; StreamingLLM and POD retain it and predict correctly, but H<sub>2</sub>O discards it due to many irrelevant tokens, resulting in an error. In case (c), the answer is in the middle; StreamingLLM cannot access it and fails, while H<sub>2</sub>O and POD both succeed. In case (d), only POD can find the answer in the “Needle in a Haystack” scenario, as the other methods overlook the answer tokens.

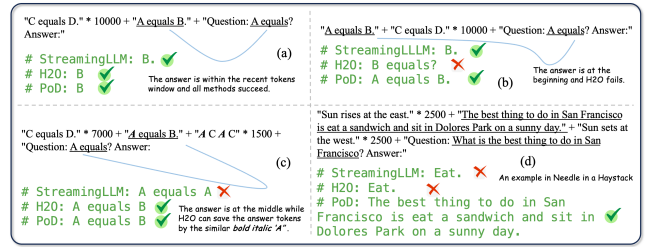


Figure 4: Case study of different methods.  $s * n$  means repeating  $n$  times of the string  $s$ .  $+$  represents the concatenation of strings.

## 4 Related Work

Long-context LLMs face significant memory challenges due to their large parameter sizes and lengthy input sequences. Existing optimization approaches for reducing KV cache memory can be broadly categorized into three areas.

**Context Compression and Computation Optimization** Many methods reduce memory usage by discarding less important tokens from the KV cache. For example, window attention (Beltagy, Peters, and Cohan 2020) retains only the most recent tokens, while LM-Infinite (Han et al. 2024) and StreamingLLM (Xiao et al. 2024) preserve both initial and recent tokens. H<sub>2</sub>O (Zhang et al. 2023) selects important tokens based on attention scores. During the prefilling phase, approaches like SnapKV (Li et al. 2024), PyramidKV (Zhang et al. 2024b), and LazyLLM (Fu et al. 2024) cache only key input tokens, while MInference (Jiang et al. 2024a) and RetrievalAttention (Liu et al. 2024c) use sparse attention to reduce latency. Some methods also directly compress input prompts (Li et al. 2023; Jiang et al. 2024b; Pan et al. 2024). Although these techniques compress the KV cache, they risk discarding critical tokens needed for later generation, which can lead to performance degradation (Tang et al. 2024).

**Hidden State Reduction and Quantization** Some other methods reduce hidden state size or quantize model weights. MQA (Shazeer 2019) and GQA (Ainslie et al. 2023) group multiple heads into one, and MLA (Liu et al. 2024a) uses low-rank representations. AWQ (Lin et al. 2024) and QLLM (Liu et al. 2024d) quantize weights and activations to save memory and computation.

**Layer Redundancy Reduction** Another line of work reduces redundancy between layers by sharing key-value states, as in LCKV (Wu and Tu 2024), CLA (Brandon et al. 2024), and MiniCache (Liu et al. 2024b). Compared to these, our method: 1) leverages attention score similarity between layers and scales this to LLMs, and 2) adopts a head-wise sharing strategy based on a search process, rather than sharing only between adjacent or final layers.

## 5 Conclusion

We present POD, a novel KV cache compression method for long-context LLMs. Unlike previous approaches that discard less important tokens, POD retains all tokens and allo-

cates memory based on token importance, using inter-layer attention redundancy to share key states for distant tokens. Experiments show that POD reduces KV cache memory by up to 35% with no loss in model performance. Our method is robust, generalizes well, and can be combined with token-selection techniques for further efficiency. We believe POD offers a practical and effective solution for memory-efficient long-context inference in LLMs.

## References

- Achiam, J.; Adler, S.; Agarwal, S.; Ahmad, L.; Akkaya, I.; Aleman, F. L.; Almeida, D.; Altschmidt, J.; Altman, S.; Anadkat, S.; et al. 2023. Gpt-4 technical report. *arXiv preprint arXiv:2303.08774*.
- Ainslie, J.; Lee-Thorp, J.; de Jong, M.; Zemlyanskiy, Y.; Lebron, F.; and Sanghai, S. 2023. GQA: Training Generalized Multi-Query Transformer Models from Multi-Head Checkpoints. In Bouamor, H.; Pino, J.; and Bali, K., eds., *Proceedings of the 2023 Conference on Empirical Methods in Natural Language Processing*, 4895–4901. Singapore: Association for Computational Linguistics.
- An, C.; Gong, S.; Zhong, M.; Zhao, X.; Li, M.; Zhang, J.; Kong, L.; and Qiu, X. 2024. L-Eval: Instituting Standardized Evaluation for Long Context Language Models. In Ku, L.-W.; Martins, A.; and Srikumar, V., eds., *Proceedings of the 62nd Annual Meeting of the Association for Computational Linguistics (Volume 1: Long Papers)*, 14388–14411. Bangkok, Thailand: Association for Computational Linguistics.
- Bai, Y.; Lv, X.; Zhang, J.; Lyu, H.; Tang, J.; Huang, Z.; Du, Z.; Liu, X.; Zeng, A.; Hou, L.; Dong, Y.; Tang, J.; and Li, J. 2024. LongBench: A Bilingual, Multitask Benchmark for Long Context Understanding. In Ku, L.-W.; Martins, A.; and Srikumar, V., eds., *Proceedings of the 62nd Annual Meeting of the Association for Computational Linguistics (Volume 1: Long Papers)*, 3119–3137. Bangkok, Thailand: Association for Computational Linguistics.
- Bairi, R.; Sonwane, A.; Kanade, A.; Iyer, A.; Parthasarathy, S.; Rajamani, S.; Ashok, B.; and Shet, S. 2024. Codeplan: Repository-level coding using llms and planning. *Proceedings of the ACM on Software Engineering*, 1(FSE): 675–698.
- Beltagy, I.; Peters, M. E.; and Cohan, A. 2020. Longformer: The Long-Document Transformer. *arXiv:2004.05150*.
- Bhojanapalli, S.; Chakrabarti, A.; Veit, A.; Lukasik, M.; Jain, H.; Liu, F.; Chang, Y.-W.; and Kumar, S. 2021. Leveraging redundancy in attention with reuse transformers. *arXiv preprint arXiv:2110.06821*.
- Brandon, W.; Mishra, M.; Nrusimha, A.; Panda, R.; and Kelly, J. R. 2024. Reducing Transformer Key-Value Cache Size with Cross-Layer Attention. *arXiv preprint arXiv:2405.12981*.
- Brown, T.; Mann, B.; Ryder, N.; Subbiah, M.; Kaplan, J. D.; Dhariwal, P.; Neelakantan, A.; Shyam, P.; Sastry, G.; Askell, A.; Agarwal, S.; Herbert-Voss, A.; Krueger, G.; Henighan, T.; Child, R.; Ramesh, A.; Ziegler, D.; Wu, J.; Winter, C.; Hesse, C.; Chen, M.; Sigler, E.; Litwin, M.; Gray, S.; Chess, B.; Clark, J.; Berner, C.; McCandlish, S.; Radford, A.; Sutskever, I.; and Amodei, D. 2020. Language Models are Few-Shot Learners. In Larochelle, H.; Ranzato, M.; Hadsell, R.; Balcan, M.; and Lin, H., eds., *Advances in Neural Information Processing Systems*, volume 33, 1877–1901. Curran Associates, Inc.
- Dubey, A.; Jauhri, A.; Pandey, A.; Kadian, A.; Al-Dahle, A.; Letman, A.; Mathur, A.; Schelten, A.; Yang, A.; Fan, A.; et al. 2024. The llama 3 herd of models. *arXiv preprint arXiv:2407.21783*.
- Fu, Q.; Cho, M.; Merth, T.; Mehta, S.; Rastegari, M.; and Najibi, M. 2024. LazyLLM: Dynamic Token Pruning for Efficient Long Context LLM Inference. *arXiv:2407.14057*.
- Gao, T.; Wettig, A.; Yen, H.; and Chen, D. 2024. How to Train Long-Context Language Models (Effectively). *arXiv:2410.02660*.
- GLM, T.; Zeng, A.; Xu, B.; Wang, B.; Zhang, C.; Yin, D.; Rojas, D.; Feng, G.; Zhao, H.; Lai, H.; et al. 2024. ChatGLM: A Family of Large Language Models from GLM-130B to GLM-4 All Tools. *arXiv preprint arXiv:2406.12793*.
- Han, C.; Wang, Q.; Peng, H.; Xiong, W.; Chen, Y.; Ji, H.; and Wang, S. 2024. LM-Infinite: Zero-Shot Extreme Length Generalization for Large Language Models. In Duh, K.; Gomez, H.; and Bethard, S., eds., *Proceedings of the 2024 Conference of the North American Chapter of the Association for Computational Linguistics: Human Language Technologies (Volume 1: Long Papers)*, 3991–4008. Mexico City, Mexico: Association for Computational Linguistics.
- Jacobs, S. A.; Tanaka, M.; Zhang, C.; Zhang, M.; Song, S. L.; Rajbhandari, S.; and He, Y. 2023. DeepSpeed ullyses: System optimizations for enabling training of extreme long sequence transformer models. *arXiv preprint arXiv:2309.14509*.
- Jiang, H.; Li, Y.; Zhang, C.; Wu, Q.; Luo, X.; Ahn, S.; Han, Z.; Abdi, A. H.; Li, D.; Lin, C.-Y.; Yang, Y.; and Qiu, L. 2024a. MInference 1.0: Accelerating Pre-filling for Long-Context LLMs via Dynamic Sparse Attention. *arXiv preprint arXiv:2407.02490*.
- Jiang, H.; Wu, Q.; Luo, X.; Li, D.; Lin, C.-Y.; Yang, Y.; and Qiu, L. 2024b. LongLLMLingua: Accelerating and Enhancing LLMs in Long Context Scenarios via Prompt Compression. In Ku, L.-W.; Martins, A.; and Srikumar, V., eds., *Proceedings of the 62nd Annual Meeting of the Association for Computational Linguistics (Volume 1: Long Papers)*, 1658–1677. Bangkok, Thailand: Association for Computational Linguistics.
- Li, Y.; Dong, B.; Guerin, F.; and Lin, C. 2023. Compressing Context to Enhance Inference Efficiency of Large Language Models. In Bouamor, H.; Pino, J.; and Bali, K., eds., *Proceedings of the 2023 Conference on Empirical Methods in Natural Language Processing*, 6342–6353. Singapore: Association for Computational Linguistics.
- Li, Y.; Huang, Y.; Yang, B.; Venkitesh, B.; Locatelli, A.; Ye, H.; Cai, T.; Lewis, P.; and Chen, D. 2024. Snapkv: Llm knows what you are looking for before generation. *arXiv preprint arXiv:2404.14469*.

- Lin, J.; Tang, J.; Tang, H.; Yang, S.; Chen, W.-M.; Wang, W.-C.; Xiao, G.; Dang, X.; Gan, C.; and Han, S. 2024. AWQ: Activation-aware Weight Quantization for On-Device LLM Compression and Acceleration. In Gibbons, P.; Pekhimenko, G.; and Sa, C. D., eds., *Proceedings of Machine Learning and Systems*, volume 6, 87–100.
- Liu, A.; Feng, B.; Wang, B.; Wang, B.; Liu, B.; Zhao, C.; Dengr, C.; Ruan, C.; Dai, D.; Guo, D.; et al. 2024a. Deepseek-v2: A strong, economical, and efficient mixture-of-experts language model. *arXiv preprint arXiv:2405.04434*.
- Liu, A.; Liu, J.; Pan, Z.; He, Y.; Haffari, G.; and Zhuang, B. 2024b. MiniCache: KV Cache Compression in Depth Dimension for Large Language Models. *arXiv preprint arXiv:2405.14366*.
- Liu, D.; Chen, M.; Lu, B.; Jiang, H.; Han, Z.; Zhang, Q.; Chen, Q.; Zhang, C.; Ding, B.; Zhang, K.; Chen, C.; Yang, F.; Yang, Y.; and Qiu, L. 2024c. RetrievalAttention: Accelerating Long-Context LLM Inference via Vector Retrieval. *arXiv:2409.10516*.
- Liu, J.; Gong, R.; Wei, X.; Dong, Z.; Cai, J.; and Zhuang, B. 2024d. QLLM: Accurate and Efficient Low-Bitwidth Quantization for Large Language Models. In *The Twelfth International Conference on Learning Representations*.
- Mazumder, S.; and Liu, B. 2024. *Lifelong and Continual Learning Dialogue Systems*. Springer.
- Menéndez, M.; Pardo, J.; Pardo, L.; and Pardo, M. 1997. The Jensen-Shannon divergence. *Journal of the Franklin Institute*, 334(2): 307–318.
- Pan, Z.; Wu, Q.; Jiang, H.; Xia, M.; Luo, X.; Zhang, J.; Lin, Q.; Rühle, V.; Yang, Y.; Lin, C.-Y.; Zhao, H. V.; Qiu, L.; and Zhang, D. 2024. LLMLingua-2: Data Distillation for Efficient and Faithful Task-Agnostic Prompt Compression. In Ku, L.-W.; Martins, A.; and Srikumar, V., eds., *Findings of the Association for Computational Linguistics ACL 2024*, 963–981. Bangkok, Thailand and virtual meeting: Association for Computational Linguistics.
- Paszke, A.; Gross, S.; Massa, F.; Lerer, A.; Bradbury, J.; Chanan, G.; Killeen, T.; Lin, Z.; Gimelshein, N.; Antiga, L.; et al. 2019. Pytorch: An imperative style, high-performance deep learning library. *Advances in neural information processing systems*, 32.
- Pope, R.; Douglas, S.; Chowdhery, A.; Devlin, J.; Bradbury, J.; Heek, J.; Xiao, K.; Agrawal, S.; and Dean, J. 2023. Efficiently scaling transformer inference. *Proceedings of Machine Learning and Systems*, 5: 606–624.
- Rajbhandari, S.; Rasley, J.; Ruwase, O.; and He, Y. 2020. ZeRO: memory optimizations toward training trillion parameter models. In *Proceedings of the International Conference for High Performance Computing, Networking, Storage and Analysis, SC '20*. IEEE Press. ISBN 9781728199986.
- Rasley, J.; Rajbhandari, S.; Ruwase, O.; and He, Y. 2020. DeepSpeed: System Optimizations Enable Training Deep Learning Models with Over 100 Billion Parameters. In *Proceedings of the 26th ACM SIGKDD International Conference on Knowledge Discovery & Data Mining, KDD '20*, 3505–3506. New York, NY, USA: Association for Computing Machinery. ISBN 9781450379984.
- Reid, M.; Savinov, N.; Teplyashin, D.; Lepikhin, D.; Lillcrap, T.; Alayrac, J.-b.; Soricut, R.; Lazaridou, A.; Firat, O.; Schrittwieser, J.; et al. 2024. Gemini 1.5: Unlocking multimodal understanding across millions of tokens of context. *arXiv preprint arXiv:2403.05530*.
- Shazeer, N. 2019. Fast transformer decoding: One write-head is all you need. *arXiv preprint arXiv:1911.02150*.
- Sheng, Y.; Zheng, L.; Yuan, B.; Li, Z.; Ryabinin, M.; Chen, B.; Liang, P.; Ré, C.; Stoica, I.; and Zhang, C. 2023. FlexGen: high-throughput generative inference of large language models with a single GPU. In *Proceedings of the 40th International Conference on Machine Learning, ICML'23*. JMLR.org.
- Soldaini, L.; Kinney, R.; Bhagia, A.; Schwenk, D.; Atkinson, D.; Authur, R.; Bogin, B.; Chandu, K.; Dumas, J.; Elazar, Y.; Hofmann, V.; Jha, A.; Kumar, S.; Lucy, L.; Lyu, X.; Lambert, N.; Magnusson, I.; Morrison, J.; Muennighoff, N.; Naik, A.; Nam, C.; Peters, M.; Ravichander, A.; Richardson, K.; Shen, Z.; Strubell, E.; Subramani, N.; Tafjord, O.; Walsh, E.; Zettlemoyer, L.; Smith, N.; Hajishirzi, H.; Beltagy, I.; Groeneveld, D.; Dodge, J.; and Lo, K. 2024. Dolma: an Open Corpus of Three Trillion Tokens for Language Model Pretraining Research. In Ku, L.-W.; Martins, A.; and Srikumar, V., eds., *Proceedings of the 62nd Annual Meeting of the Association for Computational Linguistics (Volume 1: Long Papers)*, 15725–15788. Bangkok, Thailand: Association for Computational Linguistics.
- Su, J.; Lu, Y.; Pan, S.; Murtadha, A.; Wen, B.; and Liu, Y. 2023. RoFormer: Enhanced Transformer with Rotary Position Embedding. *arXiv:2104.09864*.
- Tang, J.; Zhao, Y.; Zhu, K.; Xiao, G.; Kasikci, B.; and Han, S. 2024. QUEST: Query-Aware Sparsity for Efficient Long-Context LLM Inference. In *Forty-first International Conference on Machine Learning*.
- Team, G.; Anil, R.; Borgeaud, S.; Wu, Y.; Alayrac, J.-B.; Yu, J.; Soricut, R.; Schalkwyk, J.; Dai, A. M.; Hauth, A.; et al. 2023. Gemini: a family of highly capable multimodal models. *arXiv preprint arXiv:2312.11805*.
- Touvron, H.; Lavril, T.; Izacard, G.; Martinet, X.; Lachaux, M.-A.; Lacroix, T.; Rozière, B.; Goyal, N.; Hambro, E.; Azhar, F.; et al. 2023a. Llama: Open and efficient foundation language models. *arXiv preprint arXiv:2302.13971*.
- Touvron, H.; Martin, L.; Stone, K.; Albert, P.; Almahairi, A.; Babaei, Y.; Bashlykov, N.; Batra, S.; Bhargava, P.; Bhosale, S.; et al. 2023b. Llama 2: Open foundation and fine-tuned chat models. *arXiv preprint arXiv:2307.09288*.
- Vaswani, A.; Shazeer, N.; Parmar, N.; Uszkoreit, J.; Jones, L.; Gomez, A. N.; Kaiser, L. u.; and Polosukhin, I. 2017. Attention is All you Need. In Guyon, I.; Luxburg, U. V.; Bengio, S.; Wallach, H.; Fergus, R.; Vishwanathan, S.; and Garnett, R., eds., *Advances in Neural Information Processing Systems*, volume 30. Curran Associates, Inc.
- Wolf, T.; Debut, L.; Sanh, V.; Chaumond, J.; Delangue, C.; Moi, A.; Cistac, P.; Rault, T.; Louf, R.; Funtowicz, M.; Davison, J.; Shleifer, S.; von Platen, P.; Ma, C.; Jernite, Y.; Plu,

J.; Xu, C.; Le Scao, T.; Gugger, S.; Drame, M.; Lhoest, Q.; and Rush, A. 2020. Transformers: State-of-the-Art Natural Language Processing. In Liu, Q.; and Schlangen, D., eds., *Proceedings of the 2020 Conference on Empirical Methods in Natural Language Processing: System Demonstrations*, 38–45. Online: Association for Computational Linguistics.

Wu, H.; and Tu, K. 2024. Layer-Condensed KV Cache for Efficient Inference of Large Language Models. In Ku, L.-W.; Martins, A.; and Srikumar, V., eds., *Proceedings of the 62nd Annual Meeting of the Association for Computational Linguistics (Volume 1: Long Papers)*, 11175–11188. Bangkok, Thailand: Association for Computational Linguistics.

Xiao, G.; Tian, Y.; Chen, B.; Han, S.; and Lewis, M. 2024. Efficient Streaming Language Models with Attention Sinks. In *The Twelfth International Conference on Learning Representations*.

Xiao, T.; Li, Y.; Zhu, J.; Yu, Z.; and Liu, T. 2019. Sharing Attention Weights for Fast Transformer. In *Proceedings of the Twenty-Eighth International Joint Conference on Artificial Intelligence, IJCAI-19*, 5292–5298. International Joint Conferences on Artificial Intelligence Organization.

Xiong, W.; Liu, J.; Molybog, I.; Zhang, H.; Bhargava, P.; Hou, R.; Martin, L.; Rungta, R.; Sankararaman, K. A.; Oguz, B.; Khabsa, M.; Fang, H.; Mehdad, Y.; Narang, S.; Malik, K.; Fan, A.; Bhosale, S.; Edunov, S.; Lewis, M.; Wang, S.; and Ma, H. 2024. Effective Long-Context Scaling of Foundation Models. In Duh, K.; Gomez, H.; and Bethard, S., eds., *Proceedings of the 2024 Conference of the North American Chapter of the Association for Computational Linguistics: Human Language Technologies (Volume 1: Long Papers)*, 4643–4663. Mexico City, Mexico: Association for Computational Linguistics.

Zhang, X.; Chen, Y.; Hu, S.; Xu, Z.; Chen, J.; Hao, M.; Han, X.; Thai, Z.; Wang, S.; Liu, Z.; and Sun, M. 2024a.  $\infty$ Bench: Extending Long Context Evaluation Beyond 100K Tokens. In Ku, L.-W.; Martins, A.; and Srikumar, V., eds., *Proceedings of the 62nd Annual Meeting of the Association for Computational Linguistics (Volume 1: Long Papers)*, 15262–15277. Bangkok, Thailand: Association for Computational Linguistics.

Zhang, Y.; Gao, B.; Liu, T.; Lu, K.; Xiong, W.; Dong, Y.; Chang, B.; Hu, J.; Xiao, W.; et al. 2024b. PyramidKV: Dynamic KV Cache Compression based on Pyramidal Information Funneling. *arXiv preprint arXiv:2406.02069*.

Zhang, Z.; Sheng, Y.; Zhou, T.; Chen, T.; Zheng, L.; Cai, R.; Song, Z.; Tian, Y.; Re, C.; Barrett, C.; Wang, Z.; and Chen, B. 2023. H2O: Heavy-Hitter Oracle for Efficient Generative Inference of Large Language Models. In *Thirty-seventh Conference on Neural Information Processing Systems*.

## Impacts and Limitations

POD enables large language models to process much longer contexts with significantly reduced memory usage, without loss of performance. This makes long-context LLM deployment more practical in real-world scenarios and lowers hardware requirements for inference. The method can also be applied to various models and combined with other memory-saving techniques, supporting more efficient large-scale language model applications.

POD requires a small amount of post-training to help the model adapt to the new attention-sharing structure. While this process is lightweight compared to full model training, it still introduces extra computational cost, especially for very large models. In addition, although POD achieves strong memory savings without sacrificing accuracy, some latency overhead remains compared to the fastest token-eviction approaches, since all tokens are retained. Finally, the combination of POD with other compression or quantization techniques has not been fully explored and may present new challenges or opportunities for further efficiency improvements.

## A Baseline Details

### A.1 SnapKV

For SnapKV, we followed the official implementation<sup>§</sup>, setting the `window_size` to 4096 and using the default value 64 for `snap_kv_window_size`. Additionally, it is worth noting that we extended SnapKV to support GQA (Ainslie et al. 2023), enabling its combination with POD.

### A.2 PyramidKV

For PyramidKV, we also used the official implementation<sup>¶</sup>. The settings are: `window_sizes = 8`, `max_capacity_prompts = 2048`, `kernel_sizes = 7`, `pooling = 'maxpool'`, and `window_size = 4096`.

### A.3 Quest

For Quest, we consistently used the official codebase<sup>||</sup>, with `token_budget` set to 4096 and `chunk_size` set to 16.

### A.4 WA and WA+CPT

For window attention, we set the `window_size` parameter in FlashAttention<sup>\*\*</sup> to (4096, 0).

### A.5 StreamingLLM and LM-Infinite

Both StreamingLLM and LM-Infinite are based on the official StreamingLLM implementation<sup>††</sup>, with the position embedding adapted for each method. We set `start_size` to 16 and `recent_size` to 4080.

### A.6 H<sub>2</sub>O

H<sub>2</sub>O is based on official implementation<sup>‡‡</sup>, with `start_size` set to 96 and `recent_size` set to 4000.

### A.7 CLA

We re-implemented CLA (Brandon et al. 2024) and set the sharing factor to 2.

## B Additional Experiments

### B.1 Window Size Impact on Prediction Consistency

Window size	256	512	1024	2048	4096
Identical rate	80.3	82.2	83.6	84.8	86.0

Table 7: Proportion of identical predictions for the last 100 tokens under different recent window sizes.

To conduct this experiment, we sampled 1000 texts of length 32K from Dolma (Soldaini et al. 2024). All experiments were performed on our self-trained LLaMA3-8B-32K model. We evaluated the proportion of cases where the model predictions for the last 100 tokens were exactly the same when using only a recent window of size [256, 512, 1024, 2048, 2096], compared to using the full context. The detailed results are shown in Table 7.

<sup>§</sup><https://github.com/FasterDecoding/SnapKV>

<sup>¶</sup><https://github.com/Zefan-Cai/KVCache-Factory>

<sup>||</sup><https://github.com/mit-han-lab/Quest>

<sup>\*\*</sup><https://github.com/Dao-AILab/flash-attention>

<sup>††</sup><https://github.com/mit-han-lab/streaming-llm>

<sup>‡‡</sup><https://github.com/FMInference/H2O>

## B.2 Offline Inter-Layer Attention Sharing Exploration

We sampled 1000 sequences of length 32K from Dolma (Soldaini et al. 2024), extracting the attention scores for the last 16 tokens of each sequence. For GQA, the similarity between two layers for a group head is determined by a majority vote among the heads in that group. Figure 5 illustrates the layer sharing patterns of POD described in § 3.1.

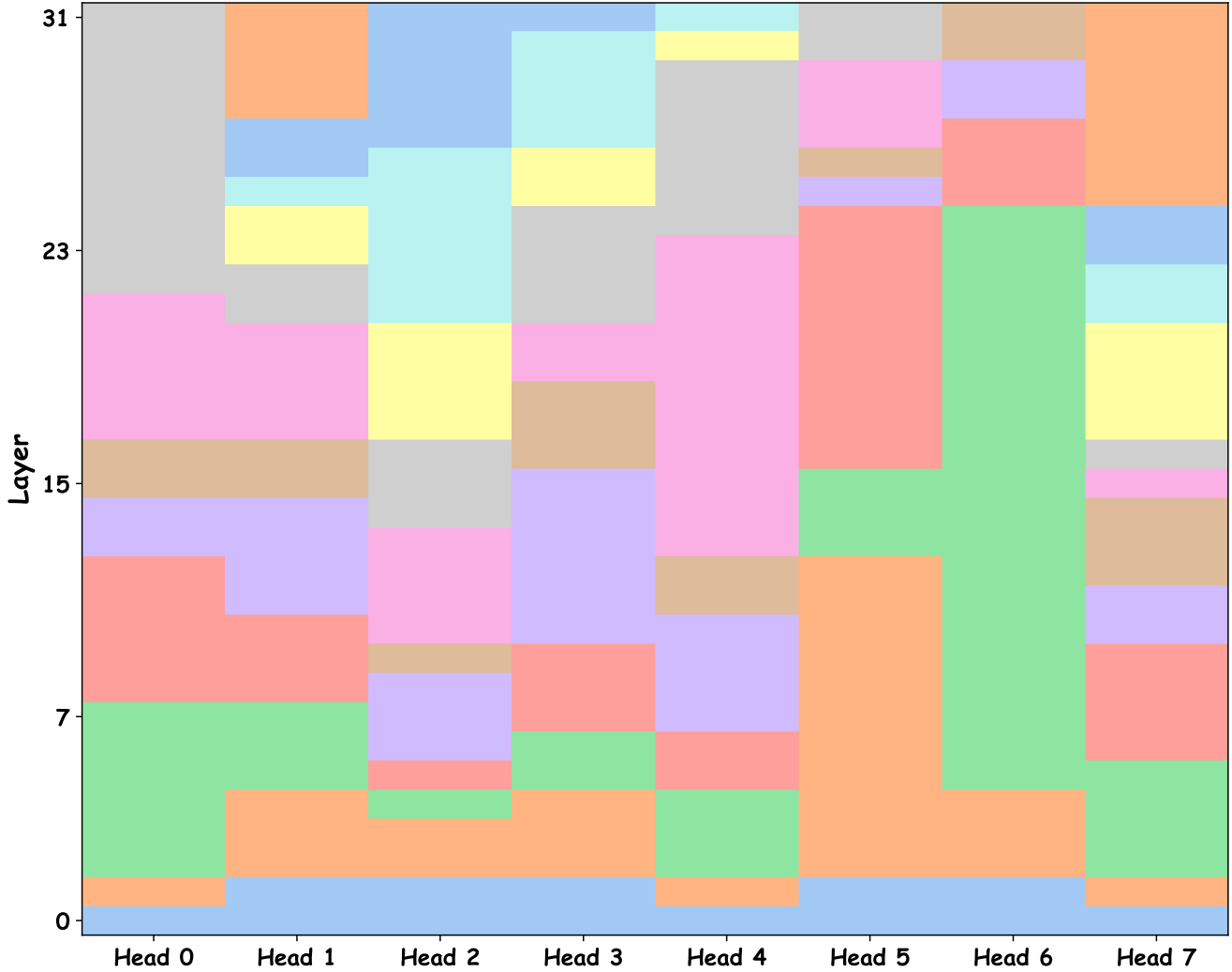


Figure 5: Offline exploration of inter-layer attention sharing for POD. Each column corresponds to a head; consecutive layers with the same color within a head indicate a group of layers that share attention. Note that the same color in different heads does not imply any relationship between those layers.

## B.3 Visual Illustration of the Search Results for Needle in a Haystack

Figure 6 provides a visual illustration of the search results for different methods. We observe that StreamingLLM and H<sub>2</sub>O fail to retrieve the needle when it falls outside their predefined window. In contrast, our method, which avoids token loss, performs comparably to dense models and is able to locate nearly all needles.

## B.4 Computation Optimization for Distant Tokens

Empirical evidence suggests that in many situations, the prediction of the next token can be effectively accomplished without attending to distant tokens. This is reflected in Equation 4, where  $g_{\ell,i}$  approaches 1 in numerous cases. Based on this, for layers within a block that are not the lowest, we can preemptively evaluate the value of  $g_{\ell,i}$ . If  $g_{\ell,i} \geq \tau$  ( $0 \leq \tau \leq 1$  is a hyperparameter), the computation of attention for distant tokens can be omitted, thereby reducing computation for distant tokens.

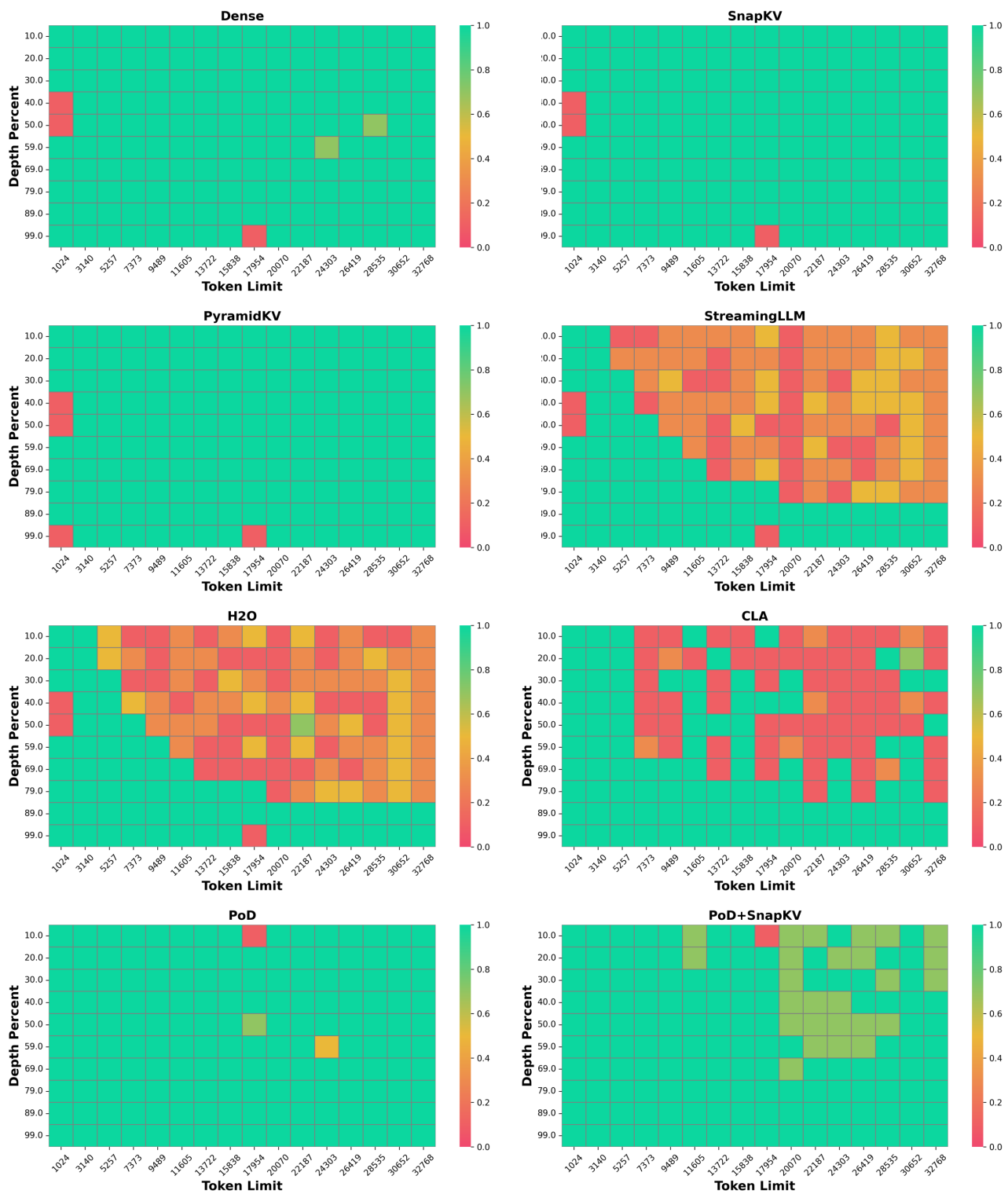


Figure 6: Visual Illustration of the Search Results for Needle in a Haystack

Figure 7 shows the relationship between the ratio of computational savings and performance loss on LEval and the value of  $\tau$ . We observe that as  $\tau$  decreases, it becomes easier to ignore the computation for distant tokens, leading to greater computational savings, but with some performance loss. However, when  $\tau < 0.7$ , the performance degradation slows down while

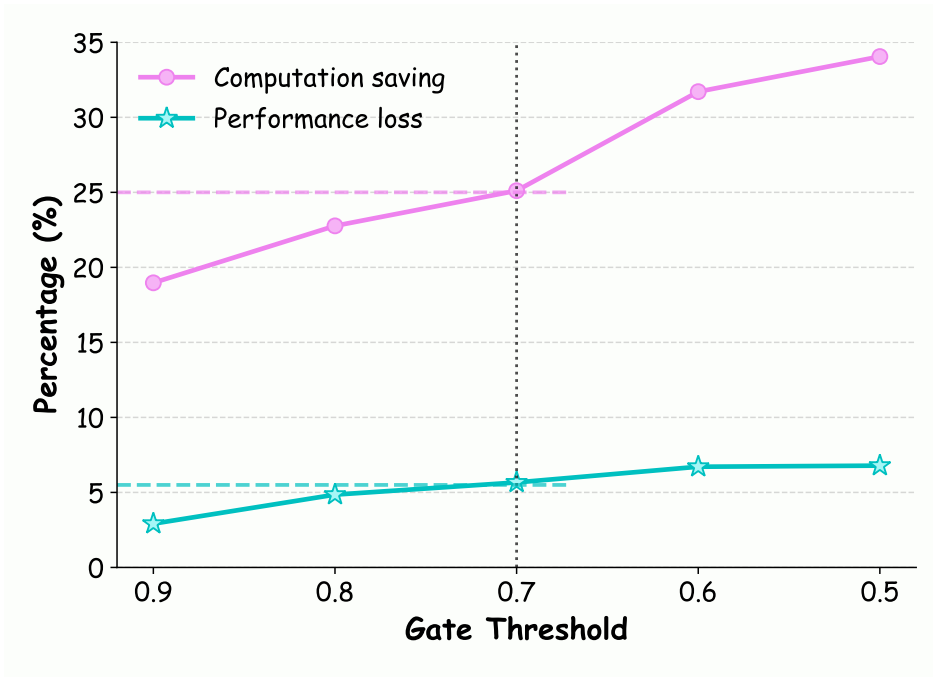


Figure 7: Computation saving and performance loss rates vs. the gate threshold  $\tau$

the computational savings become more pronounced. With  $\tau = 0.7$ , computational cost is reduced by 25% with only a 5% performance drop.

## C Theoretical Derivation

### C.1 Derivation of Integrating Attention to Proximal and Distant Tokens

For token  $x_i$  at the  $\ell$ -th layer, we divide its context tokens into two groups: proximal tokens  $T_P = \{j \mid x_j \text{ is a proximal token}\}$  and distant tokens  $T_D = \{j \mid x_j \text{ is a distant token}\}$ . The standard attention output to them is

$$\begin{aligned}
\mathbf{o}_{\ell,i} &= \frac{\sum_{j \in T_P \cup T_D} \exp \mathbf{a}_{\ell,i}^j \cdot \mathbf{V}_{\ell,j}}{\sum_{j \in T_P \cup T_D} \exp \mathbf{a}_{\ell,i}^j} \\
&= \frac{\sum_{j \in T_P} \exp \mathbf{a}_{\ell,i}^j \cdot \mathbf{V}_{\ell,j}}{\sum_{j \in T_P \cup T_D} \exp \mathbf{a}_{\ell,i}^j} + \frac{\sum_{j \in T_D} \exp \mathbf{a}_{\ell,i}^j \cdot \mathbf{V}_{\ell,j}}{\sum_{j \in T_P \cup T_D} \exp \mathbf{a}_{\ell,i}^j} \\
&= \frac{\sum_{j \in T_P} \exp \mathbf{a}_{\ell,i}^j}{\sum_{j \in T_P \cup T_D} \exp \mathbf{a}_{\ell,i}^j} \cdot \frac{\sum_{j \in T_P} \exp \mathbf{a}_{\ell,i}^j \cdot \mathbf{V}_{\ell,j}}{\sum_{j \in T_P} \exp \mathbf{a}_{\ell,i}^j} + \frac{\sum_{j \in T_D} \exp \mathbf{a}_{\ell,i}^j}{\sum_{j \in T_P \cup T_D} \exp \mathbf{a}_{\ell,i}^j} \cdot \frac{\sum_{j \in T_D} \exp \mathbf{a}_{\ell,i}^j \cdot \mathbf{V}_{\ell,j}}{\sum_{j \in T_D} \exp \mathbf{a}_{\ell,i}^j} \\
&= \frac{\sum_{j \in T_P} \exp \mathbf{a}_{\ell,i}^j}{\sum_{j \in T_P \cup T_D} \exp \mathbf{a}_{\ell,i}^j} \cdot \mathbf{o}_{\ell,i}^P + \frac{\sum_{j \in T_D} \exp \mathbf{a}_{\ell,i}^j}{\sum_{j \in T_P \cup T_D} \exp \mathbf{a}_{\ell,i}^j} \cdot \mathbf{o}_{\ell,i}^D.
\end{aligned} \tag{5}$$

Therefore, we set

$$g_{\ell,i} = \frac{\sum \exp \mathbf{a}_{\ell,i}^P}{\sum \exp \mathbf{a}_{\ell,i}^P + \sum \exp \mathbf{a}_{\ell,i}^D}. \tag{6}$$